

Structure, spectra and variability of some GPS radio sources

X. Liu^{1,*}, H. -G. Song¹, and L. Cui^{1,2}

¹ National Astronomical Observatories/Urumsq observatory, CAS, 40-5 South Beijing Rd, Urumsq 830011, PR China

² Graduate University of the Chinese Academy of Sciences, Beijing 100049, PR China

Received 2008, accepted 2008

Key words galaxies: nuclei – quasars: general – radio continuum: galaxies

We report the results of multifrequency-VLBI observations of GHz-Peaked-Spectrum (GPS) radio sources. The VLBI structure and component spectra of some GPS sources are presented. Our VLBI results show that about 80% of the GPS galaxies exhibit a compact double or CSO-like structure, while the GPS quasars tend to show a core-jet. The component spectra of the GPS galaxies are often steep/convex, and the core has a flat spectrum but it is usually hidden or weak. In addition, we studied the variability of GPS sources by comparing new flux density measures, acquired with the Urumsq 25m telescope at 4.85 GHz, with previous 87GB data. The results show that 44% of the GPS quasars varied higher than 10% in passed 20 years, while the fraction is only 12% for the GPS galaxies meaning that the GPS quasars are much more variable than GPS galaxies. In total, 25% of GPS sources show > 10% variability at 4.85 GHz in our sample.

© 2008 WILEY-VCH Verlag GmbH & Co. KGaA, Weinheim

1 Introduction

GHz-Peaked-Spectrum (GPS) radio sources are powerful ($P_{1.4\text{ GHz}} \geq 10^{25} \text{ W Hz}^{-1}$) and compact ($\leq 1 \text{ kpc}$), characterized by a convex radio spectrum that peaks between 0.3–10 GHz (observer's frame), and they represent a significant fraction ($\sim 10\%$) of the bright radio source population (O'Dea 1998). Only a few percent of them have weak extended emission (Stanghellini et al. 2005). A couple of GPS sources are also identified as Compact Symmetric Objects (CSOs, e.g. Owsianik & Conway 1998). It is believed that GPS-small sizes are most likely due to their youth ($< 10^4$ years) than to a dense confining medium (Murgia et al. 1999; O'Dea et al. 2005). In this scenario, these sources will evolve into large radio sources ($> 15 \text{ kpc}$), some of them would evolve into FR II radio sources (Fanti et al. 1995, Snellen et al. 2000). However, the GPS phenomenon is not completely understood, e.g. the distribution of sizes/ages, structure/spectra, and variability of GPS sources. We have carried out EVN (European VLBI Network) observations of 19 GPS sources, 15 of them are from the Parkes half-Jansky sample (Snellen et al. 2002) with declination $> -5^\circ$ and not observed with VLBI before (except 2121–014 and 2322–040 we observed), four others are from our previous observation list which observed with the EVN at 2.3/8.4 GHz and/or 5 GHz (Xiang et al. 2005, 2006), the 1.6 GHz observation will further provide information on the source structure and spectra. Furthermore, we have carried out flux density observations with the Urumsq 25m telescope in order to study GPS flux density variability, searching for a different behavior between galaxies and quasars.

2 VLBI structure and spectra of GPS sources

The 1.6 GHz VLBI observation was carried out on 2006 March 3 using the MK5 recording system with a bandwidth of 32 MHz and sample rate of 256 Mbps. The EVN antennae in this experiment were Effelsberg, Westerbork, Jodrell, Medicina, Noto, Onsala, Torun, Hartebeesthoek, Urumsq, and Shanghai. Snapshot observations of 19 sources (Table 1) in total of 24 hours were made. OQ208 was observed as a calibrator. The Astronomical Image Processing System (AIPS) has been used for editing, a-priori calibration, fringe fitting, self-calibration, and imaging of the data.

The results show that 12 out of 15 sources from Snellen (2002) sample exhibit compact doubles, 2 sources exhibit core-jet structure, and J1648+0242 is totally resolved out. For 4 others sources in Table 1, 3 show compact doubles, one shows a core-jet. The last six sources in Table 1 were also observed at 2.3/8.4 GHz and/or 5 GHz before this 1.6 GHz run. We summarize the VLBI structure of 19 sources in Table 1. Our results show that about 80% of the GPS galaxies exhibit a compact double or CSO like structure. The quasar J1203+0414 tends to show a core-jet. We have identified 4 CSOs from the sources which observed at 4 frequencies, according to their symmetric and steep spectrum of mini lobes. In the following we show the images and spectra of two sources as examples.

2.1 PKS 0914+114

The source has a GPS spectrum (Stanghellini et al. 1998), recently it has been optically identified as an empty field (Labiano et al. 2007). In the 1.6 GHz VLBI image, it shows a core component A, one-side jet B and two lobes C, E (Liu et al. 2007). Considering the source structure at 1.6 GHz, we

* Corresponding author: e-mail: liux@uao.ac.cn

Table 1 The GPS sources. Columns (1),(2) source names; (3) optical identification (gl: galaxy, Q: quasar, EF: empty field); (4) optical magnitude; (5) redshift (de Vries et al. 2007, those with * are photometric estimated by Tinti et al. 2005); (6) linear scale factor pc/mas [$H_0 = 71 \text{ km s}^{-1} \text{ Mpc}^{-1}$ and $q_0 = 0.5$ have been assumed]; (7) maximum angular size from the observation; (8) maximum linear size; (9) VLBI structure (cd: compact double, cj: core-jet, n: no detection); (10) low frequency spectral index; (11) higher frequency spectral index; (12) turnover frequency; (13) peak flux density; (14) references for the spectral information, 1 Snellen et al. 2002, 2 de Vries et al. 1997, 3 Stanghellini et al. 1998, where $S \propto \nu^{-\alpha}$.

1	2	3	4	5	6	7	8	9	10	11	12	13	14
<i>Name</i>	<i>other</i>	<i>id</i>	<i>m_R</i>	<i>z</i>	<i>pc/mas</i>	<i>θ</i> mas	<i>L</i> pc	<i>vlbi</i>	<i>α_l</i>	<i>α_h</i>	<i>ν_m</i> GHz	<i>S_m</i> Jy	<i>ref</i>
J0210+0419	B0208+040	gl	> 24.1	1.5*	6.1	90		cd		0.80	0.4	1.3	1
J0323+0534	4C+05.14	gl	19.2	0.1785	2.7	180	490	cd		0.85	0.4	7.1	1
J0433−0229	4C−02.17	gl	19.1	0.530	5.1	80	408	cd		0.52	0.4	3.0	1
J0913+1454	B0910+151	gl	22.9	0.47*	4.9	80		cd		0.75	0.6	1.1	1
J1057+0012	B1054+004	gl	22.3	0.65*	5.5	80?		cj		0.67	0.4	1.6	1
J1109+1043	B1107+109	gl	22.6	0.55*	5.2	60		cd		0.94	0.5	2.4	1
J1135−0021	4C−00.45	gl	21.9	0.975	6.0	120	720	cd		0.78	0.4	2.9	1
J1203+0414	B1200+045	Q	18.8	1.221	6.1	75	458	cj		0.45	0.4	1.4	1
J1352+0232	B1349+027	gl	20.0	0.607	5.4	170	918	cd		0.58	0.4	2.0	1
J1352+1107	4C+11.46	gl	21.0	0.891	5.9	50	295	cd		1.03	0.4	3.6	1
J1600−0037	B1557−004	gl				50		cd/cj		1.17	1.0	1.2	1
J1648+0242	4C+02.43	gl	22.1	0.824	5.8			n			0.4	3.4	1
J2058+0540	4C+05.78	gl	23.4	1.381	6.1	160	970	cd		0.95	0.4	3.1	1
J2123−0112	B2121−014	gl	23.3	1.158	6.1	80	488	cso	−0.56	0.75	0.4	2.0	1
J2325−0344	B2322−040	gl	23.5	1.509	6.0	75	450	cso	−0.42	0.75	1.4	1.2	1
J0917+1113	B0914+114	EF				190		cso	−0.1	1.6	0.3	2.3	3
J1753+2750	B1751+278	gl	21.7	0.86*	5.9	50		cj	−0.27	0.57	1.4	0.6	2
J1826+2708	B1824+271	gl	22.9			45		cso	−0.39	0.75	1.0	0.4	2
J2325+7917	B2323+790	gl	19.5V			32		cd	−0.3	0.75	1.4	1.2	2

Table 2 Flux densities (mJy) of VLBI components, the value with * is an upper limit. The error is $\sim 10\%$ of flux density.

Source	comp	<i>S</i> _{1.6}	<i>S</i> _{2.3}	<i>S</i> ₅	<i>S</i> _{8.4}
0914+114	A	50	38	52	19
	B	65	14	3	1*
	C	360	186	31	6
	E	40	17	10	1*
2121−014	A	594	353	196	113
	B	10*	120	14	4*
	C	415	237	107	29

have re-processed the data at 2.3, 5, 8.4 GHz with careful calibration and ‘clean’ in AIPS, the component E has been restored at 2.3, 5 GHz, and component C is restored at 8.4 GHz, as shown in Fig. 1, Fig. 2, Fig. 3.

The component spectra (Fig. 4) from the VLBI images at 1.6, 2.3, 5, and 8.4 GHz, show that the core A has a flat-spectrum than other components. The data are listed in Table 2. Based on its structure and spectra, we classify this GPS source as a CSO.

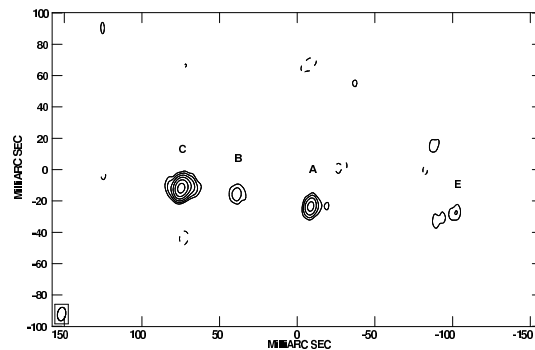


Fig. 1 0914+114 at 2.3 GHz, the restoring beam is 10.4×7.3 mas with PA -15.5° . The peak is 164 mJy/beam, the first contour is 2 mJy/beam. The contour levels here and below increase by a factor of 2.

2.2 PKS 2121−014

This GPS source is hosted by a galaxy at a redshift of 1.158. Using the VLBI results at 1.6, 2.3, 5, and 8.4 GHz we obtained the spectra for each component (Fig. 5), the two lobes A, C show steep spectra, in which we have reprocessed the 8.4 GHz data as shown in Fig. 6 with careful calibration

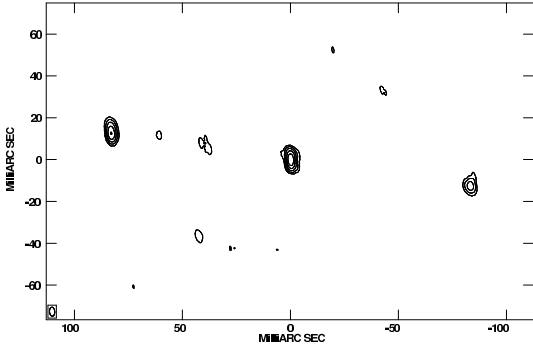


Fig. 2 0914+114 at 5 GHz, the restoring beam is 4.3×2.4 mas with PA 3.9° . The peak is 30.7 mJy/beam, the first contour is 1 mJy/beam.

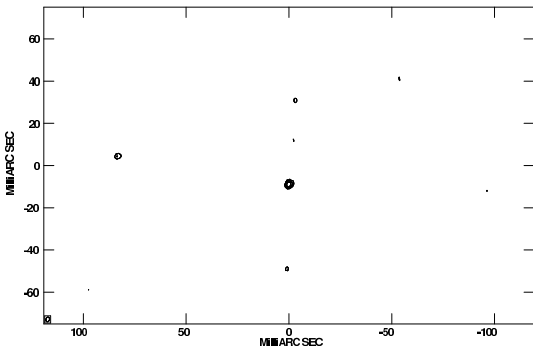


Fig. 3 0914+114 at 8.4 GHz, the restoring beam is 2.2×1.7 mas with PA -18.5° . The peak is 11.1 mJy/beam, the first contour is 1.5 mJy/beam.

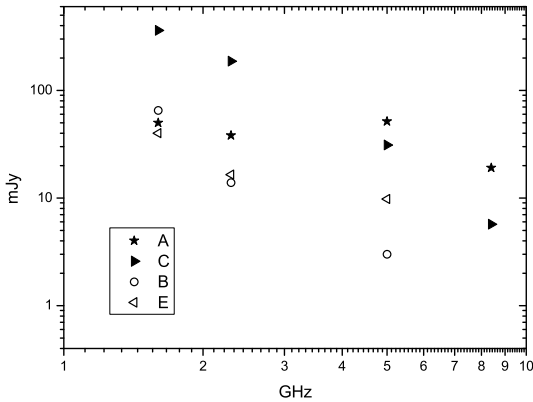


Fig. 4 Component spectra of 0914+114 at 1.6, 2.3, 5, and 8.4 GHz. Total flux density peaks at 0.3 GHz.

and ‘clean’ in AIPS. As discussed in Xiang et al. (2006), the two components A, C in the 8.4 GHz image (Xiang et al. 2005) might be swapped due to worse phase calibration, so the new image Fig. 6 is a correction. The component B as seen at 2.3, 5 GHz (Xiang et al. 2005, 2006) was not detected in this 1.6 GHz observation, assuming an upper limit of 10 mJy set by 3σ in the image, it has an inverted spectrum which is a sign of a jet or probably an absorbed core. Based on its double structure and steep spectra of lobes, we classify this GPS source as a CSO.

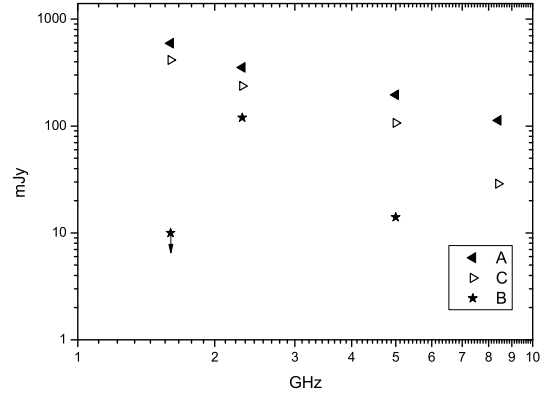


Fig. 5 Component spectra of 2121–014 at 1.6, 2.3, 5, and 8.4 GHz. Total flux density peaks at 0.4 GHz.

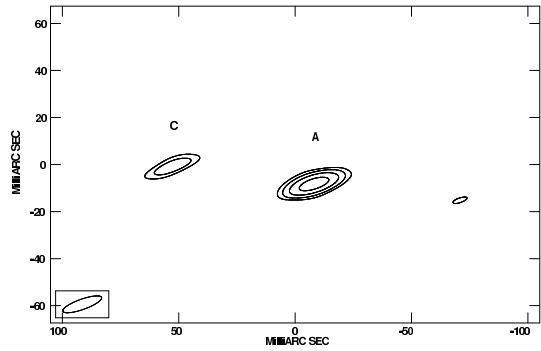


Fig. 6 2121–014 at 8.4 GHz, the restoring beam is 17.6×4.4 mas with PA -70.3° . The peak is 82.7 mJy/beam, the first contour is 7 mJy/beam.

3 Flux variability of GPS sources

It is reported that a lot of GPS sources show long term variability (Torniainen et al. 2005) especially at high radio frequency. In order to check this also at centimeter wavelength, in 2007 July, we carried out flux density measurements at 4.85 GHz for a large sample of 172 GPS sources edited by Labiano et al. (2007). By comparing these data with the 87GB and PMN data at the same frequency, we obtained the flux variations of the GPS sources between the two epoches. Because low source declination and/or bad Gaussian fits, only flux densities of 121 sources were obtained.

Flux densities were determined with ‘cross - scans’ in azimuth and elevation, fourfold in each coordinate. This enables us to check the pointing offsets in both coordinates. A Gaussian fit was performed on each sub-scan, and after applying a correction for pointing offsets the amplitudes of both AZ and EL were averaged. Then we correct the measurements for the antenna gain, and finally the flux densities were scaled to 7.55 Jy of 3C286.

As in Fig. 7, only 9 out of 73 GPS galaxies (12%) show flux variation higher than 10% ($> 2\sigma$); at the same time 21 out of 48 quasars (44%) show variability higher than 10% ($> 2\sigma$). The result indicates that GPS quasars are much more variable than GPS galaxies. The variable sources are

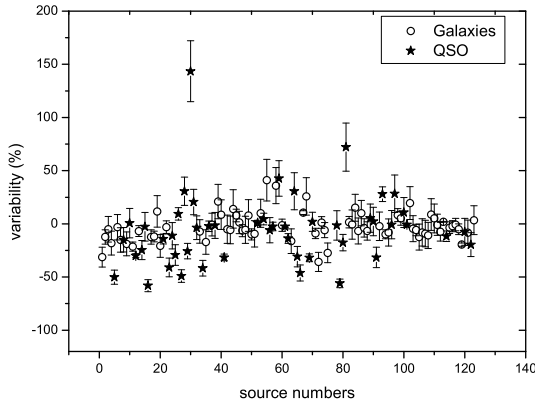


Fig. 7 Flux variation (%) at 4.85 GHz, by comparing the data measured in 2007 at Urumqi telescope with 87GB/PMN data for 121 GPS sources from Labiano et al. sample.

listed in Table 3, columns 1 to 6 are source name (1950), optical identification, 4.85 GHz flux density measured at Urumqi, 4.85 GHz flux density from 87GB or PMN data, and flux variation and the references (1: Gregory & Condon 1991; 2: Griffith et al. 1994; 3: Becker et al. 1991). Sources in Table 1 are also in Labiano sample, of them two sources show variability, the core-jet source 1054+004 shows a variation of $(11.4 \pm 3.6)\%$, and 1557–004 shows a variation of $(13.4 \pm 6.9)\%$ just at 2σ level.

4 Summary and discussion

Our VLBI results show that 80% of the GPS galaxies exhibit a compact double or CSO-like structure. However, for 13 sources which were only observed at 1.6 GHz further VLBI observations are needed for classifying their structure type in detail. Combining the 1.6, 2.3/8.4, and 5 GHz VLBI observations for other 6 sources, 4 CSOs are classified according to their steep spectrum of double lobes. The GPS galaxies are dominated by jet/lobe emission, with a hidden or weak core (it was not detected because of sensitivity in most of our sources), suggesting they are at large angles to the line of sight. While GPS quasars may be at moderate angles to the line of sight (Stanghellini et al. 2001).

Only 12% of GPS galaxies show flux variation higher than 10%, while 44% of GPS quasars show variability higher than 10% in passed 20 years. The result indicates that most GPS galaxies are stable in flux density, and the GPS quasars are much more variable than GPS galaxies. The variable GPS quasars often show compact core-jet, e.g. the quasar 0642+449 which has 140% flux variation in Fig. 7 is an extremely compact core-dominated one at a redshift of 3.4. Tornaiainen et al. (2005) found that 54% of GPS sources show flux variability in long term (with fractional variability index > 3). In our result, 25% of GPS sources show $> 10\%$ variation, the difference may be due to different samples and the definition of variability, we simply compared the flux densities in two epoches.

Table 3 Flux density variation ($> 2\sigma$) of the GPS sources.

Source	id	S_{ur}	87GB/PMN	variation	ref
0000+212	gl	242 ± 6	352 ± 47	-31.3 ± 9.3	1
0039+230	Q	820 ± 6	1645 ± 220	-50.2 ± 6.7	1
0207–224	gl	486 ± 1	618 ± 34	-21.4 ± 4.3	2
0237–233	Q	2541 ± 5	3630 ± 99	-30 ± 1.9	2
0248+430	Q	1065 ± 6	1414 ± 169	-24.7 ± 9	1
0354+231	Q	137 ± 2	327 ± 44	-58.1 ± 5.7	1
0405–280	gl	487 ± 4	553 ± 31	-11.9 ± 5.0	2
0434–188	Q	934 ± 4	1089 ± 58	-14.2 ± 4.6	2
0457+024	Q	996 ± 5	1689 ± 253	-41.0 ± 8.8	1
0507+179	Q	549 ± 5	777 ± 106	-29.3 ± 9.7	1
0621+446	Q	188 ± 3	369 ± 43	-49.1 ± 6.0	1
0636+680	Q	371 ± 17	499 ± 43	-25.7 ± 7.3	1
0642+449	Q	2900 ± 7	1191 ± 140	143.5 ± 28.6	1
0711+356	Q	525 ± 2	901 ± 113	-41.7 ± 7.3	1
0858–279	Q	1516 ± 12	2216 ± 99	-31.6 ± 3.1	2
1054+004	gl	351 ± 6	396 ± 23	-11.4 ± 3.6	2
1200+045	gl	721 ± 5	511 ± 71	41.1 ± 19.6	1
1315+415	gl	242 ± 3	178 ± 22	36.0 ± 16.9	1
1333+459	Q	853 ± 7	598 ± 70	42.6 ± 16.7	1
1354–174	Q	870 ± 5	1009 ± 54	-13.8 ± 4.6	2
1427+109	Q	855 ± 5	1236 ± 171	-30.8 ± 9.6	1
1502+036	Q	533 ± 3	991 ± 138	-46.2 ± 7.5	1
1519–273	Q	1250 ± 18	1835 ± 96	-31.9 ± 3.7	2
1543+005	gl	839 ± 5	1306 ± 182	-35.7 ± 9.0	1
1600+335	gl	1492 ± 7	2051 ± 262	-27.3 ± 9.3	1
1622+665	gl	229 ± 6	520 ± 46	-55.9 ± 4.1	1
1645+635	Q	366 ± 6	444 ± 41	-17.6 ± 7.7	1
1648+015	Q	787 ± 5	457 ± 60	72.2 ± 22.6	3
2019+050	Q	468 ± 6	684 ± 95	-31.6 ± 9.5	1
2126–158	Q	1517 ± 12	1186 ± 63	27.9 ± 6.9	2

GPS galaxies which show comparable double lobes can be interpreted as type-2 AGN in the framework of unified scheme. GPS quasars, which show a core-jet structure and variability, could be mostly type-1 AGN.

Acknowledgements. This work was supported by the National Natural Science Foundation of China (NSFC) under grant No.10773019 and the 973 Program of China under grant No.2009CB824800.

References

- Becker, R.H., White, R.L., Edwards, A.L.: 1991, *ApJS* 75, 1
- de Vries, N., Snellen, I.A.G., et al.: 2007, *A&A* 464, 879
- de Vries, W.H., Barthel, P.D., O’Dea, C.P.: 1997, *A&A* 321, 105
- Fanti, C., Fanti, R., Dallacasa, D., et al.: 1995, *A&A* 302, 317
- Gregory, P.C., Condon, J.J.: 1991, *ApJS* 75, 1011
- Griffith, M.R., Wright, A.E., et al.: 1994, *ApJS* 90, 179
- Labiano, A., Barthel, P.D., O’Dea, C.P., et al.: 2007, *A&A* 463, 97
- Liu, X., Cui, L., Luo, W.F., et al.: 2007, *A&A* 470, 97
- Murgia, M., Fanti, C., Fanti, R., et al.: 1999, *A&A* 345, 769
- O’Dea, C.P., Gallimore, J., et al.: 2005, *AJ* 129, 610
- O’Dea, C.P.: 1998, *PASP* 110, 493
- Owsianik I., Conway J.E.: 1998, *A&A* 337, 69
- Snellen, I.A.G., Lehnert, M.D., et al.: 2002, *MNRAS* 337, 981
- Snellen, I.A.G., Schilizzi, R.T., et al.: 2000, *MNRAS* 319, 445
- Stanghellini, C., Dallacasa, D., et al.: 2001, *A&A* 377, 377
- Stanghellini, C., O’Dea, C.P., et al.: 1998, *A&AS* 131, 303

- Tinti, S., Dallacasa, D., de Zotti, G., et al.: 2005, A&A 432, 31
Torniainen, I., Tornikoski, M., et al.: 2005, A&A 435, 839
Xiang, L., Dallacasa, D., Cassaro, P., et al.: 2005, A&A 434, 123
Xiang, L., Reynolds, C., Strom, R.G., et al.: 2006, A&A 454, 729